Cerebral Cortex November 2012;22:2622–2633
doi:10.1093/cercor/bhr338
Advance Access publication December 2, 2011

The Neocortical Network Representing Associative Memory Reorganizes with Time in a Process Engaging the Anterior Temporal Lobe

Ingrid L. C. Nieuwenhuis[1,2], Atsuko Takashima[1,3], Robert Oostenveld[1], Bruce L. McNaughton[4], Guillén Fernández[1,5] and Ole Jensen[1]

[1]Donders Institute for Brain, Cognition and Behaviour, Radboud University Nijmegen, 6500 HB Nijmegen, the Netherlands, [2]Sleep and Neuroimaging Laboratory, Department of Psychology, University of California, Berkeley, CA 94720-1650, USA, [3]Behavioural Science Institute, Radboud University Nijmegen, 6500 HB Nijmegen, The Netherlands, [4]Department of Neuroscience, Canadian Centre for Behavioural Neuroscience, University of Lethbridge, Lethbridge, Alberta, Canada T1K 3M4 and [5]Department of Cognitive Neuroscience, Radboud University Nijmegen Medical Centre, 6500 HB Nijmegen, the Netherlands

Address correspondence to Ingrid L. C. Nieuwenhuis, Sleep and Neuroimaging Laboratory, Department of Psychology, University of California, Berkeley, Tolman Hall 3331, Berkeley, CA 94720-1650, USA. Email: inieuwenhuis@berkeley.edu.

During encoding, the distributed neocortical representations of memory components are presumed to be associatively linked by the hippocampus. With time, a reorganization of brain areas supporting memory takes place, which can ultimately result in memories becoming independent of the hippocampus. While it is theorized that with time, the neocortical representations become linked by higher order neocortical association areas, this remains to be experimentally supported. In this study, 24 human participants encoded sets of face–location associations, which they retrieved 1 or 25 h later ("recent" and "remote" conditions, respectively), while their brain activity was recorded using whole-head magneto-encephalography. We investigated changes in the functional interactions between the neocortical representational areas emerging over time. To assess functional interactions, trial-by-trial high gamma (60–140 Hz) power correlations were calculated between the neocortical representational areas relevant to the encoded information, namely the fusiform face area (FFA) and posterior parietal cortex (PPC). With time, both the FFA and the PPC increased their functional interactions with the anterior temporal lobe (ATL). Given that the ATL is involved in semantic representation of paired associates, our results suggest that, already within 25 h after acquiring new memory associations, neocortical functional links are established via higher order semantic association areas.

Keywords: connectivity, EEG, gamma, MEG, memory consolidation

Introduction

Memories are represented in a widely distributed neural network. Different features of an event are represented by separate neocortical regions that overlap with, or possibly even correspond to, the regions that are responsible for perceiving and acting (Martin 2007). We will refer to these regions as "neocortical representational areas." The direct connectivity between these neocortical representational areas is sparse. The hippocampus, however, is reciprocally connected to a wide range of neocortical representational areas. Encoding of new episodic memories critically depends on the hippocampus (Scoville and Milner 1957). During encoding of new episodic memories, the hippocampus is thought to indirectly associate the neocortical representational areas that are collectively active during the occurrence of an event (Teyler and Discenna 1986).

With time, a reorganization of the brain areas supporting memory takes place (Alvarez and Squire 1994; Frankland and Bontempi 2005; Takashima et al. 2006; Takashima et al. 2009). Ultimately, this process can lead to memory representations, which are independent of the hippocampus (Alvarez and Squire 1994; but see Nadel and Moscovitch 1997). Thus, with time, an alternative association between the neocortical representational areas can be expected to evolve, which does not involve the hippocampus. The reorganization in the neocortical network underlying this process is, however, largely unexplored.

It is currently unclear how distant neocortical representational areas become functionally connected over time. Since direct anatomical connections between these areas are sparse, it is plausible that, for remote memory, interactions are mediated via more anatomically densely interconnected higher order association areas. The involvement of such interconnected higher order association areas in remote memory has been theorized in several forms, for example, convergence zones (Damasio 1989), the intermediate association module (McNaughton et al. 2003), or specific hub areas such as the medial prefrontal cortex (mPFC) (Frankland and Bontempi 2005) or the anterior temporal lobe (ATL) (Patterson et al. 2007). Yet, no experimental data have shown increased connectivity between the neocortical representational areas and a neocortical higher order association area emerging over time.

A recent functional magnetic resonance imaging (fMRI) study (Takashima et al. 2009) investigated functional connectivity changes in the retrieval network, over time, using Psychophysiological Interactions analysis (PPI; Friston et al. 1997). In this study, participants performed a face–location association task, meaning that they learned to associate a face to a location on the screen. Neocortical representational areas involved in this task are the fusiform face area (FFA) for faces and the posterior parietal cortex (PPC) for locations (Kanwisher et al. 1997; Takashima et al. 2007; Van der Werf et al. 2010). It was found that with time, the functional connectivity between the hippocampus and the neocortical representational areas decreased, while functional connectivity between the FFA and the PPC increased (Takashima et al. 2009). However, direct anatomical connections between the FFA and the PPC are sparse (Moeller et al. 2008), and an increased functional coupling as measured by PPI analysis does not necessarily imply a direct coupling between these regions (Friston et al. 1997). Thus, it might be more plausible that, for remote memory, interactions between the PPC and the FFA are mediated via more anatomically densely interconnected higher order association areas.

In the present study, whole-head magnetoencephalography (MEG) was used to examine time-dependent changes in

functional interactions between the neocortical representational areas and the potential emergence of intermediating higher order association areas over time. A modified version of the face–location paradigm was used (Takashima et al. 2009). Beamformer source reconstruction procedures, including realistic volume conductor models, enable sufficient spatial resolution to reliably discriminate the task relevant areas (e.g., FFA and PPC; Hämäläinen et al. 1993; Gross et al. 2001; Nolte 2003; Steinstrater et al. 2010). Additionally, the high temporal resolution of MEG enables the discrimination of oscillatory neuronal synchronization in different frequency ranges.

Electrophysiological measures of gamma activity (>30 Hz) can be valuable to study reorganization of memory networks. Gamma band synchronization has been shown to be highly important for communication between neuronal populations and to transiently link distributed cell assemblies processing related information (Singer 1999; Varela et al. 2001; Fries 2005). Systematic modulations in gamma band activity have been found during successful declarative memory encoding and retrieval (Gruber et al. 2004; Osipova et al. 2006; Nieuwenhuis et al. 2008). In addition to gamma activity, also modulations in the theta frequency range (5–7 Hz) have been observed in the neocortex associated with successful memory encoding and retrieval (Weiss et al. 2000; Sederberg et al. 2003; Osipova et al. 2006). Thus, focusing on brain signals in the frequency domain, which have been shown to be involved in linking distributed brain areas and memory, may provide novel insights in how neocortical reorganizations emerge over time.

We hypothesize that with time, the functional interactions, in the gamma and possibly theta band, between the neocortical representation areas will increase via a higher order neocortical association area. Both the ventromedial prefrontal cortex (vmPFC) and the ATL are strong candidates for becoming involved in linking the neocortical representational areas with time. The vmPFC increases in activity with time and sleep (Takashima et al. 2006; Gais et al. 2007; Sterpenich et al. 2009; Takashima et al. 2009) and has been proposed to play a linking role in remote memory (Frankland and Bontempi 2006). The ATL has been proposed to act as a hub area, linking distributed neocortical representational areas in semantic memory (Patterson et al. 2007). Additionally, the ATL is shown to be involved in the semantic representation of paired associates in general (Sakai and Miyashita 1991) and the semantic associations related to faces specifically (Brambati et al. 2010; Eifuku et al. 2010).

Materials and Methods

Subjects

Forty-one healthy right-handed subjects participated in the experiment. Thirteen subjects were excluded after the memory assessment test (see below) due to too poor memory performance. Four additional subjects were excluded after the MEG measurement due to excessive head movement (2) or because of a malfunction of the MEG system (2). The data reported are from the remaining 24 subjects (mean age: 21.21 ± 1.59 years; 12 females). None of the subjects had a history of neurological or psychiatric disorders. All subjects had normal or corrected to normal vision and gave their written consent to participate in the experiment. The study was approved by the local ethics committee.

Experimental Paradigm

The study was a within subject design, comparing brain activity during retrieval of remote (25 h) and recent (1 h) face–location associations (Fig. 1*a*). The order of the 2 conditions was counterbalanced over subjects with at least 1 week in between. Face–location associations were encoded during a training session, which took place in a behavioral lab, while recall was performed in the MEG system. Between the training session and the MEG recall, 1 and 25 h elapsed for the recent and remote conditions, respectively (Fig. 1*a*).

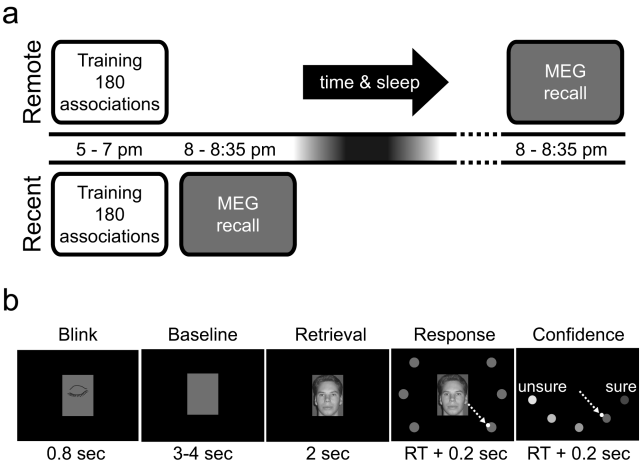

Figure 1. Behavioral setup. (*a*) In the remote condition, subjects learned 180 face–location associations starting at 5 PM. Subsequently, they went home, had a normal night of sleep, and returned to the laboratory the next evening. The next evening at 8 PM, the recall of the associations was tested during which their brain activity was measured with MEG. In the recent condition, subjects also learned 180 face–location associations, and recall followed an hour after learning. All subjects did both conditions; the order of the conditions was counterbalanced over subjects. There was at least a week time between the 2 conditions. (*b*) During the MEG recordings, each trial started with a 0.8-s period in which the subjects could blink. After that, a baseline interval (3–4 s) followed during which a gray rectangle was shown equal in size to the face stimulus. The face stimulus was then presented for 2 s during which subjects were instructed to retrieve the associated location but withhold their response. Subsequently, the 6 possible locations and the cursor (white dot) were shown, prompting the subjects to make a joystick movement to the retrieved location. Finally, the subjects had to rate the confidence of their response on a 5-point scale, again by moving the joystick, after which the next trial started.

Training Session

Subjects had to associate 180 unknown faces to 1 of 6 screen locations. The training session was identical for the recent and remote conditions, however, separate face–location sets (each 180 pairs) were used. Which set was used in each condition was counterbalanced over subjects. The associations were learned by alternating 4 "view" and 4 "test" blocks. In the view blocks, a face appeared in the center of the screen surrounded by the 6 target locations. After 1 s, one target changed color, and the face moved to that target's location where it remained visible for 2 s. Subsequently, the face disappeared, followed by a 1 s interval, after which a new face appeared. The subjects were instructed to memorize the face and the associated location. In the test blocks, faces were presented in the center of the screen together with the 6 targets, and the subjects had to actively retrieve the previously associated location. They had to indicate the recalled location by moving a joystick-controlled cursor to one of the targets. All faces were shown in random order. The training session lasted about 2 h, per condition.

MEG Recall Session

Subjects were cued with a face stimulus and had to recall the associated location, while their brain activity was measured using MEG (Fig. 1*b*). Each trial started with a blink period of 0.8 s to reduce eye-blinks later in the trial. After a jittered baseline period of 3–4 s, the face was shown in the center of the screen. The face remained on screen for 2 s, during which the subjects had to recall the associated location, while fixating on the face. After 2 s, the 6 target locations and the cursor appeared. This cued the subjects to make the response by pointing the joystick-controlled cursor to the associated location. Subsequently, the subjects had to rate the confidence of their answer on a 5-point scale. The

subjects received no feedback. When seated in the MEG system, the distance from the subjects' eyes to the screen was about 75 cm. The visual angle of the face stimulus was 4.4° by 5.7° and from center to location cues 9.2°. The recall session took about 35 min in total, per condition.

Memory Assessment

To ensure enough power for the analysis, subjects were required to encode 180 face–location associations within 2 h and be able to, later, reliably recall a large amount with high confidence. Therefore, subjects were selected prior to the experiment, on the basis of a memory assessment test, which took place at least 24 h before the start of the actual experiment. During the memory assessment test, the subjects first learned a set of 48 face-location associations, and subsequently a set of 84 face–location associations. Learning was executed identically to the training session of the actual experiment, by performing 4 view and 4 test blocks. Only subjects that had at least 74 correct answers in the last test block of the second set were selected. Thirteen of the 41 subjects did not meet the criterion. An additional benefit of the memory assessment test was that it familiarized the subjects with the training procedure used in the actual experiment, reducing the difference in learning efficiency between the 2 conditions (remote and recent). The stimuli used during the memory assessment test were not reused in the actual experiment.

Stimuli

Subjects were trained on 2 sets of 180 associations between 180 faces and 6 locations (e.g., 30 faces per location in each condition). Grayscale pictures of unknown faces with a neutral expression were used as stimuli. The pictures were taken with a digital camera in homogenous lighting conditions. The 6 target locations were arranged at equal distance around the face (Fig. 1*b*).

Data Acquisition

MEG data was acquired with a 151-sensor axial gradiometer system (CTF systems Inc., Port Coquitlam, Canada) placed in a magnetically shielded room. In addition, the horizontal and vertical electrooculograms (EOG) were recorded to later discard trials containing eye movements and blinks. The ongoing MEG and EOG signals were low-pass filtered at 300 Hz, digitized at 1200 Hz, and stored for off-line analyses. Prior to and after data acquisition, the subject's head position was determined using coils positioned at the subject's nasion and at the left and right ear canal.

Additionally, high-resolution T_1-weighted anatomical images (voxel size = 1 mm^3) of the whole brain were acquired using a 1.5-T Siemens Sonata whole-body scanner (Erlangen, Germany). These images were used for the reconstruction of individual head shapes for the source reconstruction procedures described later.

Data Analysis

Preprocessing

The data analysis was performed using the FieldTrip open source toolbox (Oostenveld et al. 2011) and Matlab 7.5 (The Mathworks Inc, August 2007). To control for a difference in recall certainties between remote and recent hits, only trials with a correct response and maximal confidence (5) were used for further analyses. Hereby, activity reflecting differences in memory strength is mitigated. Data segments contaminated with artifacts such as eye movements, eye blinks, muscle activity, and jumps in the superconducting quantum interference devices were detected with a semiautomatic routine and discarded. The synthetic third-order gradient was calculated to reduce environmental noise (Vrba and Robinson 2001). Power line noise was removed by band stop filtering around 50 Hz and harmonics.

In this experiment, an axial gradiometer MEG system was used, which does not show maximal power above the source. To simplify the interpretation of the sensor-level data, an estimate of the planar gradient was calculated for each sensor, using a nearest neighbor interpolation. The planar field gradient does typically show maximal signal power above the source (Hämäläinen et al. 1993). For source reconstruction, data from the true axial sensors and not the planar gradient estimate were used.

Time–Frequency Analysis at the Sensor Level

Previous work has shown that depending on the task, gamma band activity can range from 30 to 200 Hz. To examine which frequency band within the gamma range was involved in this specific task, time–frequency representations (TFRs) of power were obtained. To acquire a spectral smoothing of ±7.5 Hz, a multitaper approach was applied, using 3 tapers and a 0.2 s sliding time window. To enable investigation of oscillations with lower frequencies, and of theta band effects specifically, TFRs of power from 2 to 40 Hz were obtained as well. The length of sliding window was 4 cycles at each frequency ($\Delta T = 4/f$). Data were multiplied with a Hanning taper.

Source Reconstruction

Source reconstruction was performed using a frequency-domain adaptive spatial filtering algorithm (Dynamic Imaging of Coherent Sources [DICS]) (Gross et al. 2001). The DICS technique has shown to be particularly useful for the localization of oscillatory sources (Liljestrom et al. 2005). Using this method, the spatial filter, used to estimate the power at locations within the brain, based on the information present at all sensors, is constructed from the cross-spectral density matrix. To increase accuracy, a realistic single-shell volume conduction model was used (Nolte 2003). This was generated, using the subject-specific shape of the brain, based on the individual anatomical MRIs.

The locations of the sources for which the power was estimated, were aligned over subjects in Montreal Neurological Institute (MNI) space, according to the International Consortium for Brain Mapping template (MNI, Montreal, Quebec, Canada; http://www.bic.mni.mcgill.ca/brainweb). Thus, for every subject, power was estimated at the same coordinates in MNI space. This was accomplished by first making a regular spaced 3-D template grid (8 mm spacing, 6690 grid points inside the brain) based on a template MRI in MNI coordinates. Subsequently, each individual MRI was warped to the template MRI (using SPM2, http://www.fil.ion.ucl.ac.uk/spm), and the inverse of that warp was applied to the template grid. Hereby, every grid point at which power was estimated, was located in the same area of the brain in all subjects, and no interpolation in source space was necessary before averaging over subjects.

Sources were estimated for gamma power, using a 1.5 s time window and a multitaper approach. A 60–140 Hz frequency range was chosen, based on the sensor-level data in which an increase in gamma power was observed from 60 to 140 Hz with respect to the prestimulus baseline (see Results). This broadbanded gamma power was obtained by using the multitaper approach (Mitra and Pesaran 1999), this time with 119 tapers, resulting in a frequency smoothing of 100 ± 40 Hz. For each trial, sources were estimated for the poststimulus time (0–1.5 s) and the baseline (BL) period (–1.5 to 0 s) and subsequently the relative change to baseline was calculated ((poststimulus-BL)/BL). The cross-spectral density matrix, used for the filters, was the average over all trials (baseline and poststimulus) within one condition (recent or remote).

We stratified the amount of trials per condition in each subject by randomly excluding trials in the condition with most trials. This ensured that the signal-to-noise ratio of the source estimate, which depends on the averaged cross-spectral density matrix, was the same for both conditions.

For the source reconstruction of the gamma power during the 2 s retrieval time window, we used a 0.2 s sliding window and the same data as above for the filters. The relative change was calculated as above but with a baseline from –0.2 to 0 s.

Theta (4–6 Hz) sources were obtained by using a single Hanning taper, resulting in a frequency smoothing of 5 ± 1 Hz. We used the 4–6 Hz frequency range and a Hanning taper to avoid excessive smoothing and bleeding of alpha activity into the theta band.

Functional Connectivity Analysis

We used a trial-by-trial power correlation approach to study functional connectivity (Fig. 2). Brain regions that are functionally connected are expected to show a higher correlation of power fluctuations over trials

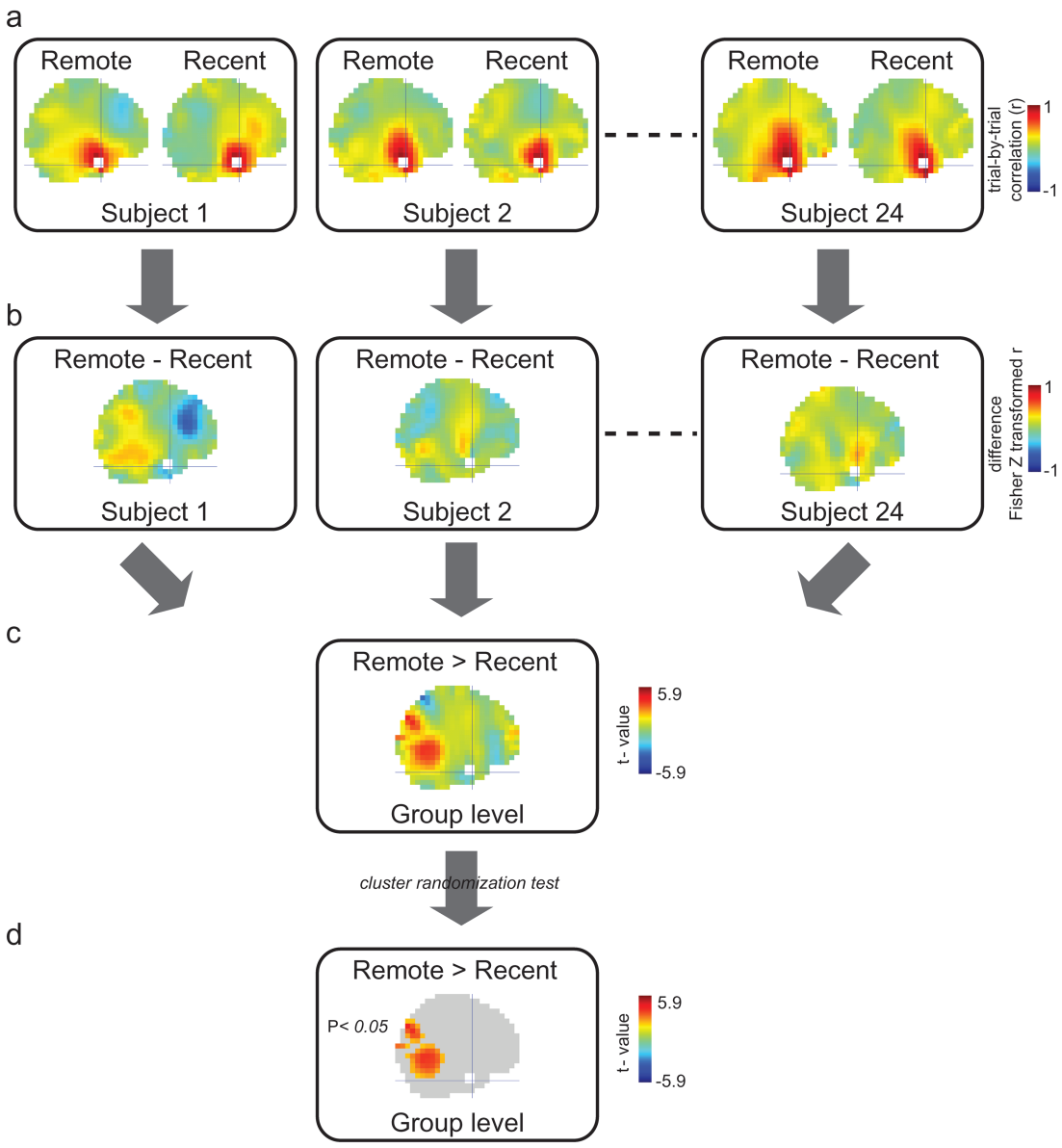

Figure 2. Trial-by-trial power correlation approach to study functional connectivity. (*a*) Within each condition in each subject, the correlation coefficient (*r*) is calculated over trials (number of trials equalized in both conditions). This is the correlation of gamma power between a predefined seed region and all grid points in the brain volume. In this figure, the left ATL was the seed region (white). The crosshair is located at the center of the seed region (MNI coordinates: [−33, 4, −41]). This results in high *r*-values at grid points close to the seed region, dropping with distance. (*b*) Because the difference bias is the same for both conditions, the difference between the Fisher *Z* transformed *r*-values shows a pattern that is interpretable as a difference in functional connectivity between conditions. (*c*) The difference between conditions is compared at group level, resulting in *t*-values showing the effect as also depicted in Supplementary Figure S3*a*. (*d*) The result after correction for multiple comparisons by cluster randomization test showing the effect as also depicted in Supplementary Figure S3*b*.

than nonconnected brain regions. First, the correlation coefficients (*r*) between the gamma activity in a predefined seed region and all grid points in the brain volume was calculated (Fig. 2*a*). As presented in Figure 2*a*, the *r* is heavily biased with the distance between the seed region and the grid point, being high for grid points close to the seed region and dropping off with increasing distance. Therefore, the value of *r* by itself cannot be interpreted as a measure of functional connectivity. However, the "difference" between the *r* in the remote and recent conditions is not biased by distance (Fig. 2*b*). This difference was calculated per subject (per grid point) and compared at group level (Fig. 2*c*,*d*) as a measure of functional connectivity (for further details, see statistical analysis).

To obtain the grid points for the FFA seed region, we defined a box in each hemisphere tightly containing the maxima of all subjects' FFA local maxima coordinates as described in Kanwisher et al. (1997) (left: center at [−36, −59, −14] MNI, box: 10 × 35 × 20 mm, resulting in 24 grid points; right: center at [40, −56, −16] MNI, box: 20 × 30 × 18 mm, resulting in 18 grid points). To obtain the grid points for the PPC seed region, we defined a sphere in each hemisphere around the local maxima as described in Takashima et al. (2007) (left: center at [−18, −76, 46] MNI, right: center at [20, −60, 54] MNI, radius: 10 mm, resulting in 8 grid points per side). To obtain the grid points for the left ATL seed region, we defined a sphere around the average of the maxima obtained by the functional connectivity analyses from FFA and from PPC as reported in the Results (center at [−33, 4, −41] MNI, radius: 10 mm, resulting in 8 grid points).

Statistical Analysis

All performed statistical tests were two sided. To quantify the difference in source power between conditions, we first calculated

t-values over trials within each subject, which were further converted to *z*-values (spm_t2z, SPM2). This procedure served to normalize the power values and to reduce the contribution of subjects with large variance. The significance of the difference in *z*-values between conditions over subjects (random effects analysis) was tested by means of the cluster randomization test incorporated in the FieldTrip software (Maris and Oostenveld 2007). This test controls the Type-1 error rate in a situation involving multiple comparisons (i.e., clustering over grid points). We used 10 000 randomizations to obtain the Monte Carlo *P* value.

In the functional connectivity analysis, we computed the between trial correlations (Pearson) within each condition (per grid point) and subsequently compared the Fisher *Z* transformed correlation coefficients (Jenkins and Watts 1968) by a paired *t*-test over subjects (Fig. 2*c*). Hereby, we are separating task-induced power fluctuations from the experimentally manipulated functional connectivity. The results with FFA and PPC as seed region in both the theta and the gamma band and with the left ATL seed region in the theta band were uncorrected $P < 0.005$, minimum cluster size: 5 consecutive grid points. The gamma band result with the left ATL as seed region was corrected for multiple comparisons by means of the randomization test (Maris and Oostenveld 2007).

Results

Behavioral Results

At the end of the training, subjects correctly recalled 92% of the face–location associations (recent: mean = 92%, standard deviation (SD) = 9%; remote: mean = 92%, SD = 11%). As expected, there were no differences after the initial training in accuracy, confidence, or reaction time between the remote and the recent conditions (Table 1). After the 1- and 25- h intervals, recall was tested again while brain activity was recorded by MEG. Performance was slightly better in the recent condition, as reflected by higher accuracy (recent: mean hits = 88%, SD = 12%; remote: mean hits = 84%, SD = 15%; paired *t*-test $P = 0.0013$), higher confidence ratings for the correct responses (recent: mean = 4.7, SD = 0.2; remote: mean = 4.6, SD = 0.3; paired *t*-test $P = 0.0005$), and a higher occurrence of fully confident hits (recent: mean = 76%, SD = 20%; remote: mean = 67%, SD = 23%; paired *t*-test $P = 0.0002$).

Theta and High Gamma Band Activity Increases during Associational Recall

To examine which frequency ranges are involved during retrieval (independent of remote/recent condition), the data were characterized by means of spectral analyses. First, we characterized the gamma power modulation during the retrieval period compared with the prestimulus baseline. During retrieval, gamma power increased with respect to baseline in a frequency range from 60 to 140 Hz (Fig. 3*a*). A clear broadband increase of gamma was most prominent in sensors over occipital areas, but it extended to sensors over temporal and parietal cortex. Given that the increase in gamma band activity primarily occurred in the 60–140 Hz range for both recent and remote recall, we constrained the rest of the analysis to this frequency band. The sources of the high gamma activity were reconstructed independently for each condition using a beamformer approach (Gross et al. 2001) (Fig. 3*b*). During the retrieval period (from 0 to 1.5 s), there was a robust increase of gamma power compared with the prestimulus baseline ($t = -1.5$ to 0 s; remote $P < 0.0001$; recent $P < 0.0001$; Monte Carlo *P* value, corrected for multiple comparisons). The difference was dominated by an extended source including visual, parietal (including the PPC), posterior temporal (including the FFA), and left motor cortex.

Additionally, TFRs of power were calculated for the lower frequencies (Supplementary Fig. S1). In both conditions, a task related increase was found in the theta band (4–6 Hz), which was strongest over the frontal and temporal sensors.

Table 1
Behavioral results

	Training		MEG recall	
	Recent mean (SD)	Remote mean (SD)	Recent mean (SD)	Remote mean (SD)
Hits (%)	92 (9)	92 (11)	88 (12)	84 (15)*
Conf hits	4.7 (0.3)	4.7 (0.3)	4.7 (0.2)	4.6 (0.3)*
Conf misses	2.6 (1.1)	2.6 (1.0)	2.9 (0.8)	2.7 (0.8)
Fully conf hits (%)	79 (20)	79 (20)	76 (20)	67 (23)*
RT hits (s)	1.67 (0.38)	1.65 (0.27)	—	—
RT misses (s)	3.70 (2.83)	3.64 (1.89)	—	—

Note: Conf = confidence rating (5 = fully confident), RT = reaction time.
*Significant difference between remote and recent conditions ($P < 0.01$).

Gamma Power Correlations Increase with Time between the FFA and the ATL, and the PPC and the ATL

Next, we set out to examine the power correlations in the gamma band amongst the neocortical representational areas (FFA: faces, PPC: locations), comparing remote with recent recall. The gamma band correlations increased with the passage of time between the FFA seed region (both hemispheres pooled, as defined by Kanwisher et al. 1997) and the left ATL (MNI coordinates maximum [–42, 0, –42]; *t*-test, $P = 0.0012$ uncorrected, 18 grid points), the mPFC (MNI coordinates maximum [2, 52, 14]; *t*-test, $P = 0.0017$ uncorrected, 9 grid points), and the brainstem (MNI coordinates maximum [2, –14, –28]; *t*-test, $P = 0.0003$ uncorrected, 14 grid points; Fig. 4*a*, and Supplementary Fig. S2*a,b*).

When using the PPC as seed region (both hemispheres pooled, as found by Takashima et al. 2007), the gamma band correlations only increased with respect to the left ATL (MNI coordinates maximum [–24, 8, –44]; *t*-test, $P = 0.0028$ uncorrected, 5 grid points; Fig. 4*b*, and Supplementary Fig. S2*c,d*). The gamma band correlations showed a time-dependent decrease between the PPC and the left and right paracentral lobule (MNI coordinates maximum [8, –32, 60]; *t*-test, $P = 0.0008$ uncorrected, 9 grid points) and the left precuneus (MNI coordinates maximum [–12, –48, 36]; *t*-test, $P = 0.0019$ uncorrected, 6 grid points; Supplementary Fig. S2*c,d*).

With respect to a lenient statistical threshold ($P < 0.005$ uncorrected), both the FFA and the PPC showed a higher correlation of gamma activity with the left ATL in the remote condition. The identified left ATL areas were largely overlapping (see Supplementary Fig.S1*a,c*). Therefore, we subsequently used the left ATL (10 mm sphere with the center point defined by the mean location of the grid points identified as maxima, for further details, see Materials and Methods) as seed region (Fig. 5 and Supplementary Fig. S3*a,b*). A robust time-dependent increase in correlation was found between the left ATL and a cluster of brain regions (multiple comparison corrected, Monte Carlo *P* value = 0.0370). The cluster included the left FFA, the right PPC, the right inferior occipital cortex, the bilateral superior occipital cortex, and the right cerebellum. In conclusion, when seeding in either the PPC or the FFA, the ATL emerges as the region that shows increased functional interactions over time. In reverse, when

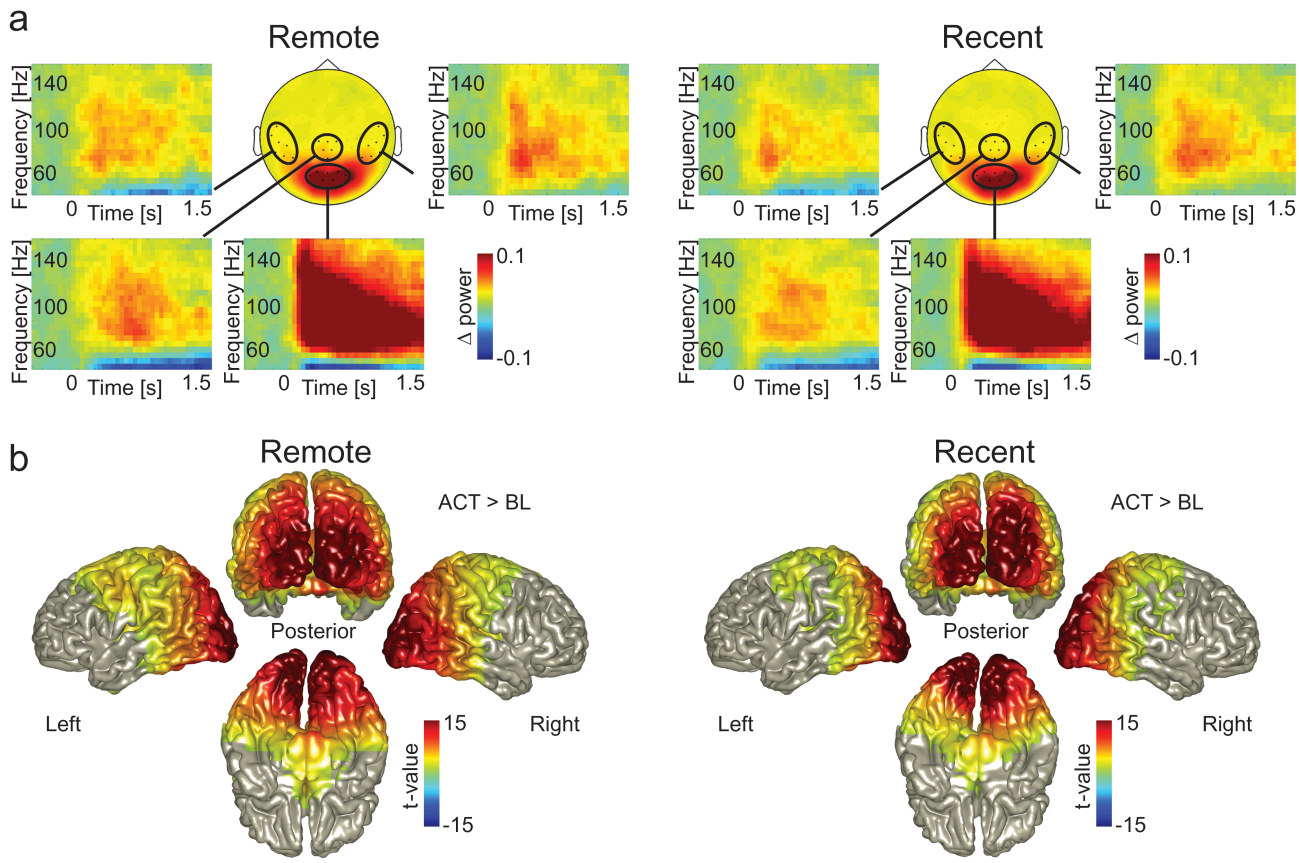

Figure 3. Gamma band activity during retrieval of face–location associations. (*a*) The topography (circular plot; $f = 60$–140 Hz) and TFRs of the grand-average gamma power for both conditions. The TFRs were averaged over the encircled channels. For visualization of the task related effect, gamma power is shown relative to a baseline period ($t = -1.4$ to -0.1 s). Note that the increase in gamma power is broadbanded and sustained. (*b*) Source level gamma power ($f = 60$–140 Hz, $t = 0$ to 1.5 s) was significantly increased compared with baseline ($t = -1.5$ to 0 s) in occipital, parietal, posterior temporal, and motor areas in both conditions. The increase was significant on group level (corrected for multiple comparisons).

seeding in the ATL, the functional interactions with a specific cluster of brain areas, including the PPC and FFA, increase with time. These results support a specific increase in functional interactions emerging over time between the neocortical representational areas and the ATL.

We also examined how the source level gamma power developed during the 2 s retrieval time window. We focused on the power at the grid points of the left ATL, the left FFA, and the right PPC (Fig. 5, bottom right). The gamma power peaked first in the FFA around 0.3 s and then in the PPC around 0.6 s. This is in line with the FFA first being engaged by the face, followed by activation of the PPC when retrieving the associated location. Interestingly, gamma power in the left ATL did not show a clear increase compared with prestimulus baseline levels during the retrieval period.

Additionally, changes in functional interactions between the FFA, the PPC, and the ATL were investigated in the theta (4–6 Hz) frequency band. The right superior orbitofrontal cortex and left cerebellum showed an increase over time in their correlations with the FFA (Supplementary Table 1, Supplementary Fig. S4*a*,*b*). The PPC showed an increase over time in its correlations with the right cerebellum and a time-dependent decrease with the right superior parietal cortex (Supplementary Table 1, Supplementary Fig. S4*c*,*d*). Importantly, no region was found that showed a change over time in its correlations with both the FFA and the PPC. When using the left ATL seed region that was identified in the high gamma band, only areas were found showing a decrease over time in their correlations with the ATL, that is, the right supramarginal cortex and right superior frontal cortex (Supplementary Table 1, Supplementary Fig. S4*e*,*f*). Importantly, neither the FFA nor the PPC showed a change in correlations over time with this area. Additionally, no changes were significant after correction for multiple comparisons using cluster randomization testing. In summary, the increase in functional interactions with time between the left ATL and the neocortical representational areas FFA and PPC was specific to the high gamma band and not present in the theta range.

No Time-Dependent Changes in Gamma Power in Left ATL, FFA, and PPC

To exclude that differences in power between conditions are the cause of the observed differences in correlation between the conditions, we also compared high gamma power (60–140 Hz) between the remote and the recent conditions. Gamma power was higher for the remote condition (multiple comparison corrected, Monte Carlo P value = 0.0256), however, the cluster of brain regions showing this difference was not the same as the brain regions showing a difference in gamma power correlation. Stronger gamma power was found in the superior occipital areas (bilaterally, more strongly on the

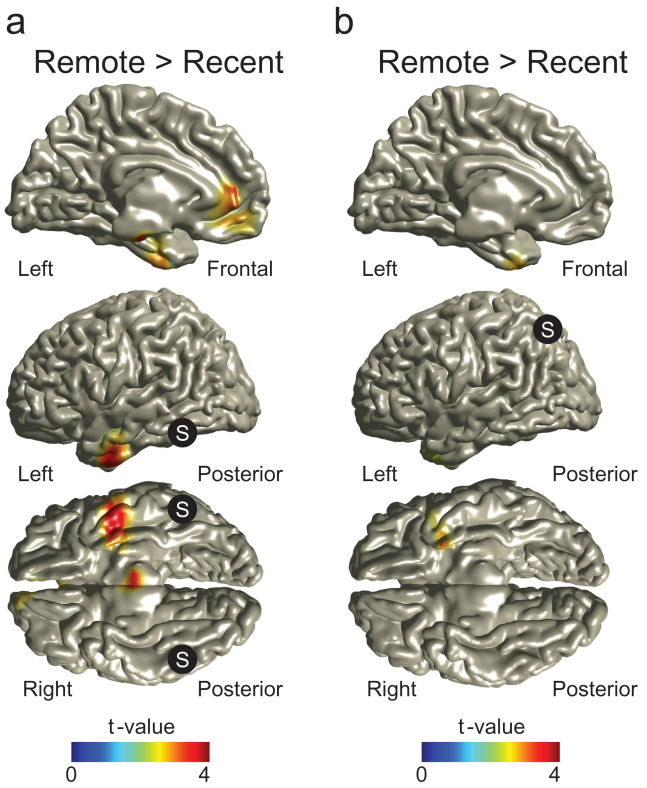

Figure 4. Correlation difference between conditions, with FFA and PPC as seed regions. (*a*) Correlation difference between conditions of source-reconstructed gamma power (f = 60–140 Hz) fluctuations between the FFA (bilateral; MNI coordinates: [−36, −59, −14] [40, −56, −16], S in picture) and the rest of the brain. The correlation increased between the FFA and the left ATL for the remote compared with the recent condition. *T*-values with $P > 0.05$ uncorrected were masked out for illustrational purposes. For *t*-values with $P < 0.005$, see Supplementary Figure S2*b*. (*b*) Correlation difference between conditions of source-reconstructed gamma power (f = 60–140 Hz) fluctuations between the PPC (bilateral; MNI coordinates: [−18, −76, 46] [20, −60, 54], S in picture) and the rest of the brain. The correlation increased between the PPC and the left ATL in the remote compared with the recent condition. *T*-values with $P > 0.05$ uncorrected were masked out for illustrational purposes. For *t*-values with $P < 0.005$, see Supplementary Figure S2*d*.

left side), left cuneus and precuneus, left superior parietal cortex, and inferior and middle temporal gyrus (bilaterally, more strongly on the right side) (Fig. 6). We also explicitly tested whether there were power differences that might explain the increasing power–power correlations over time between the left FFA, the left ATL, and the right PPC. Therefore, we first defined grid points that showed a strong correlation effect ($P < 0.005$ uncorrected) and subsequently calculated the mean power per condition over these grid points in these areas. Finally, the difference between the remote and the recent conditions was compared using a 2-tailed paired *t*-test. No task-dependent difference in gamma power was found in the left ATL (8 grid points; $P = 0.6341$), the left FFA (20 grid points; $P = 0.4177$), or the right PPC (10 grid points; $P = 0.8071$). In summary, gamma "power" in the left ATL, FFA, and PPC did not significantly increase with time, in contrast to gamma "power correlations" which did increase with time between these areas.

Discussion

We have conducted an MEG study in which we investigated the consequences of off-line time on the neocortical network representing face–location memory associations. We applied a connectivity analysis based on power–power correlations in the theta and gamma band between the neocortical brain regions known to be involved in face–location memory (i.e., the FFA and PPC). Both when using the FFA and when using the PPC as seed regions, high gamma power (60–140 Hz) fluctuations over trials correlated more in the remote compared with the recent condition, with an overlapping area in the left ventral ATL. When using that ATL area as seed region, this revealed a robust enhancement of the functional interactions over time with a cortical network including the FFA and PPC. These interactions were specific to the high gamma frequency band. This indicates that, during the 25 h following learning, a substantial reorganization takes place in the neocortical network representing associative memories. With the passage of time, our data suggest that the ATL starts functioning as a linking area between the neocortical representational areas FFA and PPC.

We considered a time-dependent increase in high gamma band power correlations over trials, between sources, as evidence of an increase in functional connectivity. An increase in correlated activity does not necessarily imply an increase in functional connectivity. Additional factors that would lead to an increase in correlation have to be excluded. First, merely power increases in brain regions involved in the task could also lead to increased power–power correlations due to a larger signal-to-noise ratio. However, the network of areas showing a power increase over time (Fig. 6) was different from the network showing increases in correlation (Fig. 5). The largest time-dependent power increase was observed in occipital brain areas, while the power in FFA, PPC, ATL did not significantly increase with time. Therefore, it seems unlikely that the observed time-dependent increases in power–power correlations are caused by mere power increases.

Another explanation for an increase in power–power correlations could be a common source driving the FFA, PPC, and ATL, which is not detected in the MEG signals. However, this explanation is not very likely since the array of MEG sensors covered the whole head, and a sophisticated individualized volume conduction model was used, resulting in reliable source estimation in neocortical parts of the brain (Nolte 2003). Even though we cannot exclude a deep common source below the neocortex, driving the FFA, PPC, and ATL, no such area was found in an fMRI study using a similar face–location task (Takashima et al. 2009). Additionally, there are no likely candidates apparent from the literature. Summarizing, we conclude that the observed time-dependent increases in power–power correlations between the ATL and the FFA and between the ATL and the PPC most likely are explained by an increase in functional connectivity between these regions.

We have used the correlation of source-reconstructed trial-by-trial gamma power fluctuations between brain areas as a measure of functional connectivity. Although phase synchronization between distant brain regions is a theoretically attractive mechanism for connectivity between brain region (Engel et al. 2001; Varela et al. 2001; Fries 2005), we have not used this measure in our MEG study. Due to the low signal-to-noise ratio of noninvasive recordings of electrophysiological events, the reliability of the phase estimate is a concern. Additionally, a reliable phase estimate of broadband signals, like the high gamma band response from 60 to 140 Hz we showed in our study, is problematic. The power correlations (or envelope correlations) in broad frequency bands can, however, be estimated robustly

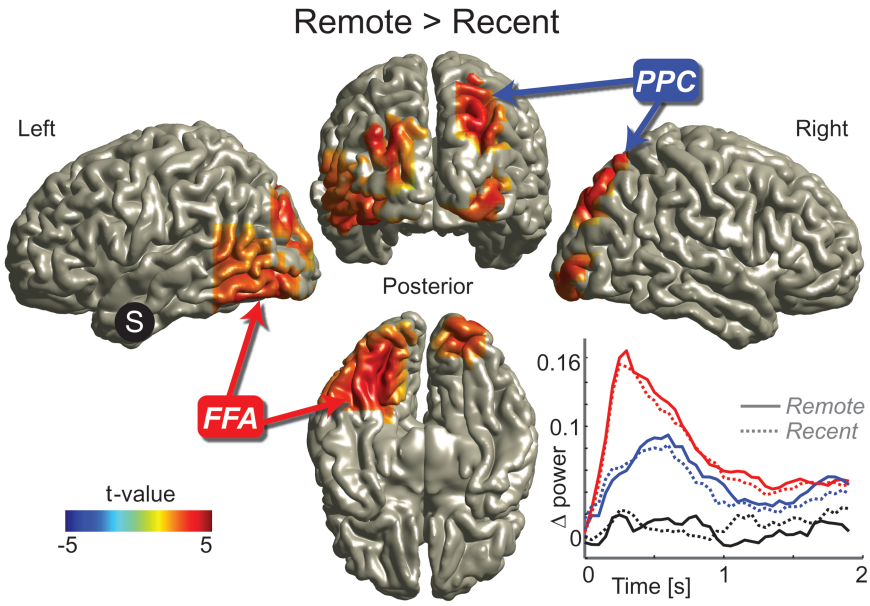

Figure 5. Increased correlations in the gamma band in the remote condition between the left ATL and a cluster of brain regions including the FFA and PPC. The correlation difference between conditions of source-reconstructed gamma power (f = 60–140 Hz) fluctuations between the left ATL (MNI coordinates: [−33, 4, −41], S in picture) and the rest of the brain was calculated. The correlation increased in the remote compared with the recent condition between left ATL and a series of brain regions including left FFA and right PPC. The difference between conditions is significant after correcting for multiple comparisons. Only significant clusters are shown; for unmasked data, see Supplementary Figure S3*a*. Inset, below right: Time course of source-reconstructed gamma power (f = 60–140 Hz) relative to the baseline period (t = −0.2 to 0 s) in the left FFA (red), the right PPC (blue), and the left ATL (black). Note that the power in the FFA peaks first, followed by the power in the PPC. There is no significant difference in power between the remote and the recent condition in all 3 areas.

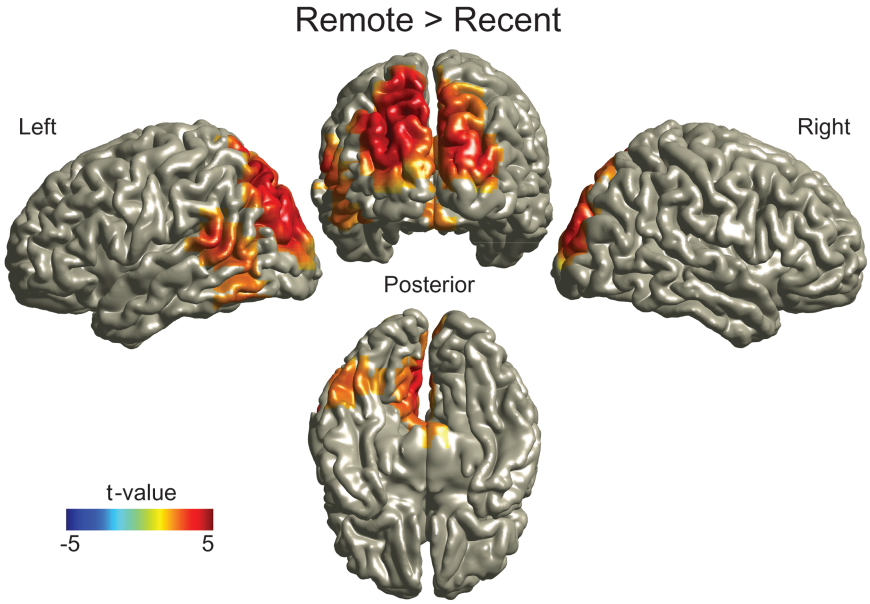

Figure 6. Source reconstruction of the differences in gamma power (f = 60–140 Hz) between the remote and the recent conditions. Gamma power was significantly increased in the remote condition in the visual, parietal, and temporal areas. Note that the areas shown to differ in functional connectivity with the left ATL as shown in Figure 5 do not show a significant difference in gamma power between conditions. Difference between conditions is significant after correcting for multiple comparisons, Monte Carlo P value = 0.0256.

(Bruns et al. 2000). Finally, the existence of power–power correlations does by no means preclude phase synchronization.

The approach of using trial-by-trial power correlation has been shown to be a valuable tool for investigating functional connectivity in both intracranial recordings from human epileptic patients (Lachaux et al. 2005) and other MEG studies (de Lange et al. 2008; Mazaheri et al. 2009; de Pasquale et al. 2010). In this study, we take the approach a step further by considering power correlations between "sources" reconstructed in the brain volume. Performing the connectivity analysis at source level is a crucial step in our analysis. First, it allowed us to separate the contribution of multiple sources that project to the same sensors, making the procedure more sensitive and more interpretable (Schoffelen and Gross 2009).

Especially, the activity of the deeper ventral areas would be difficult to identify at sensor level. At sensor level, the signals from these sources would be mixed with activity from other brain regions. Second, using subject-specific realistic head models allowed us to take individual head positions and anatomical differences into account (Nolte 2003; Steinstrater et al. 2010). This also made it possible to transform the individual source data to MNI space, enabling us to use the known anatomical coordinates of the areas of interest (FFA and PPC) in the connectivity analysis. The beamforming approach to source localization has been used in numerous studies, many of which have been reproduced and provided results that are compatible with direct intracranial measurements in animals (e.g., Osipova et al. 2006; de Lange et al. 2008; Fries et al. 2008; Nieuwenhuis et al. 2008; Mazaheri et al. 2009; Van der Werf et al. 2010).

A strong indication supporting the validity of our approach is the specificity that emerged when seeding in different areas. When seeding in either the FFA or the PPC, the ATL stood out as the region becoming more connected over time. When seeding in ATL, specifically the FFA and PPC emerged. In summary, we believe that the trial-by-trial power correlation approach on source level is useful and robust for revealing changes in functional connectivity in MEG data. Note that power–power correlations do not preclude phase synchronization as being the underlying mechanism for the changes in connectivity (Varela et al. 2001; Fries 2005), however, power–power correlations appear to be a more sensitive method.

The reported increases in functional interactions between the ATL and both the FFA and the PPC were specific to the high gamma (60–140 Hz) band and not present in the theta (4–6 Hz) range. This is consistent with a growing body of intracranial studies in patients, as well as local field potential recordings in macaque monkeys supporting the case that cognitive processing is reflected in modulations of power in the broadband frequency range greater than 60 Hz extending up to 200 Hz (Edwards et al. 2005; Ray et al. 2008; Crone et al. 2009; Hamamé et al. 2012). Traditionally, studies of gamma band activity emphasized frequencies in the 30–90 Hz range (Gray et al. 1989; Fries et al. 2001). Although the neuronal mechanisms underlying high gamma activity are debated (Miller et al. 2009), the difference in response to stimuli in studies using electrocorticography indicates that low and high gamma activity have independent physiological origins (Crone et al. 2009). High gamma band activity in the local field potential is strongly coupled with the neuronal firing rate, more so than low gamma power (Ray et al. 2008).

A recent fMRI study, using a similar face–location task, reported a time-dependent increase in functional connectivity, assessed by a PPI analysis, between the FFA and the PPC directly, not via the ATL (Takashima et al. 2009). However, direct anatomical connections between the FFA and the PPC are sparse (Moeller et al. 2008). Moreover, a PPI analysis that results in 2 areas being functionally connected, does not exclude the possibility of the ATL being an uncaptured region, driving this functional connectivity. The ATL could have been missed because of susceptibility artifacts in the blood oxygen level–dependent (BOLD) signal, caused by the proximity of air-filled sinuses (Binney et al. 2010). Especially the most ventral part of the ATL, which we identified in this study, is liable to these kinds of artifacts (Weiskopf et al. 2006; Visser et al. 2010). Additionally, in the fMRI study by Takashima et al. (2009), the most ventral part of the ATL was not captured in some subjects (personal communication with A. Takashima), which could have lead to reduced sensitivity in this area. Furthermore, it has been shown that the fMRI BOLD signal and the MEG gamma signal are sensitive to different aspects of neuronal activity (Herrmann and Debener 2008; Muthukumaraswamy and Singh 2008). The functional interaction we report may only be detectable in the high gamma range, while the BOLD signal contains contributions from the combined activity over larger frequency ranges (Herrmann and Debener 2008). This stresses the need for using complementary neuroimaging techniques, to optimally reveal the many aspects of brain activity.

When studying changes in memory over time, it is important to be aware of possibly confounding differences between the remote and the recent conditions, which are not related to memory. To avoid that changes over time would be confounded by nonspecific effects such as retrieval effort, the current study was designed to have a high recall rate for both remotely and recently encoded associations. Additionally, one might argue that the reported changes with time are explained by changes in stimulus processing. However, in a previous study using a similar face–location task (Takashima et al. 2007), the PPC was selectively activated while retrieving location memory during the presentation of a face cue and not during recognition of faces that were not previously associated with a location. Therefore, we believe that the reported increased functional interaction between the ATL and both the FFA and the PPC, which was observed while only the face stimulus was presented without any location cues, is more likely to be a true memory effect.

A similar face–location paradigm has been used in a behavioral study in which subjects were not overtrained to the same extent as in the current study (Talamini et al. 2008). In this experiment, robust behavioral effects were identified after both a 12- and a 24- h sleep interval. We thus believe that it is likely that the reported neocortical reorganization of the retrieval network is accompanied by behavioral changes even after only one night of sleep. Incidentally, we are not claiming that the reorganization process is completed in 25 h. What we have demonstrated is that a spontaneous reorganization of the interactions among neocortical memory–related brain areas is measurable within the first 25 h after learning. This is in line with existing literature showing that time-dependent changes can be captured within a few days (Wagner et al. 2004; Ellenbogen et al. 2007; Tse et al. 2007; Talamini et al. 2008).

In our experiment, the ATL did not display an increased gamma power compared with the resting baseline, neither in the remote nor in the recent condition. This does not mean, however, that the ATL was not active or engaged. Other studies have shown that contrasting the activation of the ventral anterior temporal regions with resting baseline activity does not reveal a strong difference. This suggests that semantic processing occurs during resting conditions, reducing the possibility of detecting task-modulated neuronal activity in the ATL (Binder et al. 1999; Binney et al. 2010). Importantly, the overall lack of task-dependent power modulation does not prevent the possibility of assessing changes in functional connectivity. Due to the selective difference between the remote and the recent conditions in the functional interactions of ATL with the FFA and PPC, the involvement of the ATL emerged from the connectivity analysis in our study.

In summary, our data suggest that within 25 h after encoding, a higher order neocortical association area starts to

link the neocortical representational areas, as has been theorized (Damasio 1989; McNaughton et al. 2003; Patterson et al. 2007). In our experiment, this association area turned out to be the left ventral part of the ATL. Given that the ATL is anatomically connected to many representational areas, for example, the inferior temporal cortex (which includes the FFA) and the PPC (Webster et al. 1994; Blaizot et al. 2010), it is suited for linking these areas. These findings are in line with experiments on patients with semantic dementia and computational models, which have proposed the ATL to be the area that links neocortical representational areas in order to form semantic memories, that is, to act as a domain-general hub (McClelland and Rogers 2003; Patterson et al. 2007; Lambon Ralph et al. 2010). Interestingly, the specific part of the ATL that has been found to be crucial for semantic representations matches the area we found in this study: the anterior "ventral" parts of the (left) ATL (Binney et al. 2010; Visser et al. 2010).

The ATL has also been shown to be involved in representing paired associative memory. In the ATL of monkeys, single neurons were found to respond to either of 2 abstract patterns that were previously associated in a training phase (Sakai and Miyashita 1991). Recently, it was shown that cells in the ventral anterior inferior temporal cortex in monkeys responded both to faces and to abstract patterns, and the majority of these neurons responded selectively to a particular associative pair (Eifuku et al. 2010). These ATL neurons most likely receive inputs from neurons in representational areas involved in coding the individual stimuli of the paired associates. Thus the observed data are compatible with the notion that the ATL serves to link representations. The ATL seems specifically involved in pairing semantic information to "face" stimuli (Simmons et al. 2010; Brambati et al. 2010; Eifuku et al. 2010). In a recent human fMRI study, the left ATL was shown to functionally interact with the FFA during the retrieval of specific semantic information related to a familiar face (Brambati et al. 2010).

Other regions besides the FFA, PPC, and ATL might become involved in the retrieval network over time. The mPFC is an area of interest because this area has also been proposed to take over the linking role of the hippocampus with the passage of time (Frankland and Bontempi 2005; Takashima et al. 2006; Van Kesteren et al. 2010). We did find an increase in the functional interactions between the FFA and the mPFC. The identified mPFC area overlapped with the vmPFC, which has been found to become more engaged over time and sleep (Takashima et al. 2006; Gais et al. 2007; Sterpenich et al. 2009), although the maximum activity was more dorsal in our case. However, we did not find an increase in functional connectivity between the PPC and the mPFC. In line with previous studies, our data suggest that the mPFC might become more involved with the passage of time, although they do not show strong evidence that this area starts linking the neocortical representational areas in remote memory (Nieuwenhuis and Takashima 2011).

The stage is now set for further investigation of the role of the ATL with the aging of memories. An increasing amount of studies points to the importance of the ATL in semantic memory representation (Sakai and Miyashita 1991; Patterson et al. 2007; Binney et al. 2010; Brambati et al. 2010; Eifuku et al. 2010; Lambon Ralph et al. 2010; Visser et al. 2010). Additionally, it has been suggested that with the passage of time, a reorganization of memory representations might take place from being detailed and episodic into a more efficient, nonoverlapping, generalized, and structured code, resulting in a "semanticization" of the information (McClelland et al. 1995; Wiltgen et al. 2004; Patterson et al. 2007; Stickgold 2009). It is conceivable that this semanticization occurring with the aging of memories is partly achieved by the formation of links between the neocortical representational areas, through higher order semantic association areas including the ATL. Many questions remain, emphasizing the need to directly explore the role of the ATL in semanticization and the representation of remote memory. In particular, experiments in which the time-dependent semanticization is related to the degree of ATL engagement could elucidate this.

Supplementary Material

Supplementary material can be found at: http://www.cercor.oxfordjournals.org/

Funding

This work was supported by grants from the Dutch National Science Foundation (grant numbers NWO 051-04-100 and NWO 451-06-006), National Institute of Mental Health (grant number MH046823), the Alberta Heritage Foundation for Medical Research, and the BrainGain Smart Mix Programme of the Netherlands Ministry of Economic Affairs and the Netherlands Ministry of Education, Culture and Science, and a stipend from the Niels Stensen Stichting.

Notes

We thank Jan Mathijs Schoffelen for assistance during data analysis and Penny Lewis for constructive comments on the manuscript. *Conflict of Interest*: None declared.

References

Alvarez P, Squire LR. 1994. Memory consolidation and the medial temporal-lobe—a simple network model. Proc Natl Acad Sci U S A. 91:7041–7045.

Binder JR, Frost JA, Hammeke TA, Bellgowan PSF, Rao SM, Cox RW. 1999. Conceptual processing during the conscious resting state: a functional MRI study. J Cogn Neurosci. 11:80–93.

Binney RJ, Embleton KV, Jefferies E, Parker GJ, Lambon Ralph MA. 2010. The ventral and inferolateral aspects of the anterior temporal lobe are crucial in semantic memory: evidence from a novel direct comparison of distortion-corrected fMRI, rTMS, and semantic dementia. Cereb Cortex. 20:2728–2738.

Blaizot X, Mansilla F, Insausti AM, Constans JM, Salinas-Alaman A, Pro-Sistiaga P, Mohedano-Moriano A, Insausti R. 2010. The human parahippocampal region: I. Temporal pole cytoarchitectonic and MRI correlation. Cereb Cortex. 20:2198–2212.

Brambati SM, Benoit S, Monetta L, Belleville S, Joubert S. 2010. The role of the left anterior temporal lobe in the semantic processing of famous faces. Neuroimage. 53:674–681.

Bruns A, Eckhorn R, Jokeit H, Ebner A. 2000. Amplitude envelope correlation detects coupling among incoherent brain signals. Neuroreport. 11:1509–1514.

Crone NE, Sinai A, Korzeniewska A. 2009. Cortical function mapping with intracranial EEG. In: Tong S, Thakor NV, editors. Quantitative EEG analysis methods and application. Norwood (MA): Artech House. p. 369–399.

Damasio A. 1989. The brain binds entities and events by multiregional activation from convergence zones. Neural Comput. 1:123–132.

de Lange FP, Jensen O, Bauer M, Toni I. 2008. Interactions between posterior gamma and frontal alpha/beta oscillations during imagined actions. Front Hum Neurosci. 2:7.

de Pasquale F, Della Penna S, Snyder AZ, Lewis C, Mantini D, Marzetti L, Belardinelli P, Ciancetta L, Pizzella V, Romani GL, et al. 2010.

Temporal dynamics of spontaneous MEG activity in brain networks. Proc Natl Acad Sci U S A. 107:6040–6045.
Edwards E, Soltani M, Deouell LY, Berger MS, Knight RT. 2005. High gamma activity in response to deviant auditory stimuli recorded directly from human cortex. J Neurophysiol. 94:4269–4280.
Eifuku S, Nakata R, Sugimori M, Ono T, Tamura R. 2010. Neural correlates of associative face memory in the anterior inferior temporal cortex of monkeys. J Neurosci. 30:15085–15096.
Ellenbogen JM, Hu PT, Payne JD, Titone D, Walker MP. 2007. Human relational memory requires time and sleep. Proc Natl Acad Sci U S A. 104:7723–7728.
Engel AK, Fries P, Singer W. 2001. Dynamic predictions: oscillations and synchrony in top-down processing. Nat Rev Neurosci. 2: 704–716.
Frankland PW, Bontempi B. 2005. The organization of recent and remote memories. Nat Rev Neurosci. 6:119–130.
Frankland PW, Bontempi B. 2006. Fast track to the medial prefrontal cortex. Proc Natl Acad Sci U S A. 103:509–510.
Fries P. 2005. A mechanism for cognitive dynamics: neuronal communication through neuronal coherence. Trends Cogn Sci. 9:474–480.
Fries P, Reynolds JH, Rorie AE, Desimone R. 2001. Modulation of oscillatory neuronal synchronization by selective visual attention. Science. 291:1560–1563.
Fries P, Scheeringa R, Oostenveld R. 2008. Finding gamma. Neuron. 58:303–305.
Friston KJ, Buechel C, Fink GR, Morris J, Rolls E, Dolan RJ. 1997. Psychophysiological and modulatory interactions in neuroimaging. Neuroimage. 6:218–229.
Gais S, Albouy G, Boly M, Dang-Vu TT, Darsaud A, Desseilles M, Rauchs G, Schabus M, Sterpenich V, Vandewalle G, et al. 2007. Sleep transforms the cerebral trace of declarative memories. Proc Natl Acad Sci U S A. 104:18778–18783.
Gray CM, Konig P, Engel AK, Singer W. 1989. Oscillatory responses in cat visual-cortex exhibit inter-columnar synchronization which reflects global stimulus properties. Nature. 338:334–337.
Gross J, Kujala J, Hamalainen M, Timmermann L, Schnitzler A, Salmelin R. 2001. Dynamic imaging of coherent sources: studying neural interactions in the human brain. Proc Natl Acad Sci U S A. 98:694–699.
Gruber T, Tsivilis D, Montaldi D, Muller MM. 2004. Induced gamma band responses: an early marker of memory encoding and retrieval. Neuroreport. 15:1837–1841.
Hämäläinen M, Hari R, Ilmoniemi RJ, Knuutila J, Lounasmaa OV. 1993. Magnetoencephalography—theory, instrumentation, and applications to noninvasive studies of the working human brain. Rev Mod Phys. 65:413–497.
Hamamé CM, Vidal JR, Ossandon T, Jerbi K, Dalal SS, Minotti L, Bertrand O, Kahane P, Lachaux JP. 2012. Reading the mind's eye: online detection of visuo-spatial working memory and visual imagery in the inferior temporal lobe. Neuroimage. 59:872–879.
Herrmann CS, Debener S. 2008. Simultaneous recording of EEG and BOLD responses: a historical perspective. Int J Psychophysiol. 67:161–168.
Jenkins GM, Watts DG. 1968. Spectral analysis and its applications. Boca Raton (FL): Emerson-Adams.
Kanwisher N, McDermott J, Chun MM. 1997. The fusiform face area: a module in human extrastriate cortex specialized for face perception. J Neurosci. 17:4302–4311.
Lachaux JP, George N, Tallon-Baudry C, Martinerie J, Hugueville L, Minotti L, Kahane P, Renault B. 2005. The many faces of the gamma band response to complex visual stimuli. Neuroimage. 25:491–501.
Lambon Ralph MA, Sage K, Jones RW, Mayberry EJ. 2010. Coherent concepts are computed in the anterior temporal lobes. Proc Natl Acad Sci U S A. 107:2717–2722.
Liljestrom M, Kujala J, Jensen O, Salmelin R. 2005. Neuromagnetic localization of rhythmic activity in the human brain: a comparison of three methods. Neuroimage. 25:734–745.
Maris E, Oostenveld R. 2007. Nonparametric statistical testing of EEG- and MEG-data. J Neurosci Methods. 164:177–190.
Martin A. 2007. The representation of object concepts in the brain. Annu Rev Psychol. 58:25–45.
Mazaheri A, Nieuwenhuis ILC, van Dijk H, Jensen O. 2009. Prestimulus alpha and mu activity predicts failure to inhibit motor responses. Hum Brain Mapp. 30:1791–1800.
McClelland JL, McNaughton BL, Oreilly RC. 1995. Why there are complementary learning-systems in the hippocampus and neocortex—insights from the successes and failures of connectionist models of learning and memory. Psychol Rev. 102:419–457.
McClelland JL, Rogers TT. 2003. The parallel distributed processing approach to semantic cognition. Nat Rev Neurosci. 4:310–322.
McNaughton BL, Barnes CA, Battaglia FP, Bower MR, Cowen SL, Ekstrom AD, Gerrard JL, Hoffman KL, Houston FP, Karten Y, et al. 2003. Off-line reprocessing of recent memory and its role in memory consolidation: a progress report. In: Maquet P, Smith C, Stickgold R, editors. Sleep and brain plasticity. New York (NY): Oxford University Press. p. 225–246.
Miller KJ, Sorensen LB, Ojemann JG, den Nijs M. 2009. Power-law scaling in the brain surface electric potential. PLoS Comput Biol. 5:e1000609.
Mitra PP, Pesaran B. 1999. Analysis of dynamic brain imaging data. Biophys J. 76:691–708.
Moeller S, Freiwald WA, Tsao DY. 2008. Patches with links: a unified system for processing faces in the macaque temporal lobe. Science. 320:1355–1359.
Muthukumaraswamy SD, Singh KD. 2008. Spatiotemporal frequency tuning of BOLD and gamma band MEG responses compared in primary visual cortex. Neuroimage. 40:1552–1560.
Nadel L, Moscovitch M. 1997. Memory consolidation, retrograde amnesia and the hippocampal complex. Curr Opin Neurobiol. 7:217–227.
Nieuwenhuis ILC, Takashima A. 2011. The role of the ventromedial prefrontal cortex in memory consolidation. Behav Brain Res. 218:325–334.
Nieuwenhuis ILC, Takashima A, Oostenveld R, Fernández G, Jensen O. 2008. Visual areas become less engaged in associative recall following memory stabilization. Neuroimage. 40:1319–1327.
Nolte G. 2003. The magnetic lead field theorem in the quasi-static approximation and its use for magnetoencephalography forward calculation in realistic volume conductors. Phys Med Biol. 48:3637–3652.
Oostenveld R, Fries P, Maris E, Schoffelen JM. 2011. FieldTrip: open source software for advanced analysis of MEG, EEG, and invasive electrophysiological data. Comput Intell Neurosci. 2011:156869.
Osipova D, Takashima A, Oostenveld R, Fernández G, Maris E, Jensen O. 2006. Theta and gamma oscillations predict encoding and retrieval of declarative memory. J Neurosci. 26:7523–7531.
Patterson K, Nestor PJ, Rogers TT. 2007. Where do you know what you know? The representation of semantic knowledge in the human brain. Nat Rev Neurosci. 8:976–987.
Ray S, Crone NE, Niebur E, Franaszczuk PJ, Hsiao SS. 2008. Neural correlates of high-gamma oscillations (60-200 Hz) in macaque local field potentials and their potential implications in electrocorticography. J Neurosci. 28:11526–11536.
Sakai K, Miyashita Y. 1991. Neural organization for the long-term-memory of paired associates. Nature. 354:152–155.
Schoffelen JM, Gross J. 2009. Source connectivity analysis with MEG and EEG. Hum Brain Mapp. 30:1857–1865.
Scoville WB, Milner B. 1957. Loss of recent memory after bilateral hippocampal lesions. J Neurol Neurosurg Psychiatry. 20:11–21.
Sederberg PB, Kahana MJ, Howard MW, Donner EJ, Madsen JR. 2003. Theta and gamma oscillations during encoding predict subsequent recall. J Neurosci. 23:10809–10814.
Simmons WK, Reddish M, Bellgowan PS, Martin A. 2010. The selectivity and functional connectivity of the anterior temporal lobes. Cereb Cortex. 20:813–825.
Singer W. 1999. Neuronal synchrony: a versatile code for the definition of relations? Neuron. 24:49–65.
Steinstrater O, Sillekens S, Junghoefer M, Burger M, Wolters CH. 2010. Sensitivity of beamformer source analysis to deficiencies in forward modeling. Hum Brain Mapp. 31:1907–1927.

Sterpenich V, Albouy G, Darsaud A, Schmidt C, Vandewalle G, Vu TTD, Desseilles M, Phillips C, Degueldre C, Balteau E, et al. 2009. Sleep promotes the neural reorganization of remote emotional memory. J Neurosci. 29:5143–5152.
Stickgold R. 2009. How do I remember? Let me count the ways. Sleep Med Rev. 13:305–308.
Takashima A, Nieuwenhuis ILC, Jensen O, Talamini LM, Rijpkema M, Fernandez G. 2009. Shift from hippocampal to neocortical centered retrieval network with consolidation. J Neurosci. 29:10087–10093.
Takashima A, Nieuwenhuis ILC, Rijpkema M, Petersson KM, Jensen O, Fernández G. 2007. Memory trace stabilization leads to large-scale changes in the retrieval network: a functional MRI study on associative memory. Learn Mem. 14:472–479.
Takashima A, Petersson KM, Rutters F, Tendolkar I, Jensen O, Zwarts MJ, McNaughton BL, Fernández G. 2006. Declarative memory consolidation in humans: a prospective functional magnetic resonance imaging study. Proc Natl Acad Sci U S A. 103:756–761.
Talamini LM, Nieuwenhuis ILC, Takashima A, Jensen O. 2008. Sleep directly following learning benefits consolidation of spatial associative memory. Learn Mem. 15:233–237.
Teyler TJ, Discenna P. 1986. The hippocampal memory indexing theory. Behav Neurosci. 100:147–154.
Tse D, Langston RF, Kakeyama M, Bethus I, Spooner PA, Wood ER, Witter MP, Morris RGM. 2007. Schemas and memory consolidation. Science. 316:76–82.
Van der Werf J, Jensen O, Fries P, Medendorp WP. 2010. Neuronal synchronization in human posterior parietal cortex during reach planning. J Neurosci. 30:1402–1412.
Van Kesteren MTR, Rijpkema M, Ruiter DJ, Fernandez G. 2010. Retrieval of associative information congruent with prior knowledge is related to increased medial prefrontal activity and connectivity. J Neurosci. 30:15888–15894.
Varela F, Lachaux JP, Rodriguez E, Martinerie J. 2001. The brainweb: phase synchronization and large-scale integration. Nat Rev Neurosci. 2:229–239.
Visser M, Embleton KV, Jefferies E, Parker GJ, Lambon Ralph MA. 2010. The inferior, anterior temporal lobes and semantic memory clarified: novel evidence from distortion-corrected fMRI. Neuropsychologia. 48:1689–1696.
Vrba J, Robinson SE. 2001. Signal processing in magnetoencephalography. Methods. 25:249–271.
Wagner U, Gais S, Haider H, Verleger R, Born J. 2004. Sleep inspires insight. Nature. 427:352–355.
Webster MJ, Bachevalier J, Ungerleider LG. 1994. Connections of inferior temporal areas teo and te with parietal and frontal-cortex in macaque monkeys. Cereb Cortex. 4:470–483.
Weiskopf N, Hutton C, Josephs O, Deichmann R. 2006. Optimal EPI parameters for reduction of susceptibility-induced BOLD sensitivity losses: a whole-brain analysis at 3 T and 1.5 T. Neuroimage. 33:493–504.
Weiss S, Muller HM, Rappelsberger P. 2000. Theta synchronization predicts efficient memory encoding of concrete and abstract nouns. Neuroreport. 11:2357–2361.
Wiltgen BJ, Brown RAM, Talton LE, Silva AJ. 2004. New circuits for old memories: the role of the neocortex in consolidation. Neuron. 44:101–108.